Desalination and Water Treatment
www.deswater.com

21 (2010) 202–209
September

1944-3994/1944-3986
doi: 10.5004/dwt.2010.1490

Preparation, characterization and photocatalytic activity of a novel nanostructure ZnO composite film derived sol-gel process using organic binder materials

Mojtaba Nasr-Esfahani[a]*, Ali Khakifirooz[b], Nahid Tavakoli[c], Mohammad Hassan Soleimani[c]

[a]*Department of Materials Science and Engineering, Islamic Azad University-Najafabad Branch, Najafabad, 517, Iran*
Tel. +983112356771; Fax +983112356771; email: m-nasresfahani@iaun.ac.ir
[b]*Research Center, Institute of Standard and Industrial Research of Iran, Karaj, Iran*
[c]*Payam Noor University, Isfahan, Iran*

Received 17 August 2009; accepted 11 February 2010

ABSTRACT

A novel sol–gel-derived zinc oxide nanostructure has been prepared by spin-coating and investigated for the purpose of producing films. ZnO films were spin-coated on microscope glass slides via methylcellulose (MC) aided sol–gel route using zinc acetate–acetic acid–EtOH as starting materials and heat treatment. Scanning electron microscopy (SEM) investigations showed that relatively dense, crack-free and transparent ZnO composite films, as well as, a decrease in the size of the ZnO nanoparticles, were achieved via the MC assisted sol–gel and single-step deposition at room temperature. Fourier transform infrared spectroscopy (FTIR) and thermal gravimetry analysis (TGA) results demonstrated full decomposition of the organic materials after firing. Photocatalytic activity of the composite films were evaluated through the degradation of a textile dye, Acid Blue R (C.I. Acid Blue 92) as a model pollutant and were compared with those of similar composite film without MC. 2%MC/ZnO thin film showed an interesting decolorization performance, as denoted by an attenuation degree of 99% and decoloration rate, assuming an apparent first order reaction, reaching 9.8×10^{-2} min^{-1}.

Keywords: Decolorization; Sol–gel; Acid Blue R; Nanostructure; ZnO composite film; Methylcellulose

1. Introduction

Dye pollutants are an important source of environmental concern. The release of wastewater containing dye in the ecosystem is a dramatic source of aesthetic pollution and perturbations in aquatic life [1,2]. Most of the organic dyes are not easily degradable by standard biological methods. Methods such as adsorption on activated carbon, ultrafiltration, reverse osmosis, coagulation, ion exchange and oxidation with peroxide are usually applied efficiently. Nevertheless, they do not destruct the pollutant molecule [3]. Recently, the efficiency of advanced oxidation processes (AOP) for the degradation of recalcitrant compounds has been extensively used. The key advantage of this degradation method is that it can be carried out under ambient conditions and lead to complete mineralization of organic carbon. In pursuit of a better method for the

*Corresponding author

detoxification of coloured wastewater, heterogeneous photocatalysis stands uppermost. Many researchers have been attempting the photocatalytic degradation of dyes [4,5] using various photocatalysts, mainly with TiO_2/UV system. However, the important shortcoming of TiO_2 semiconductor is that it absorbs only a small portion of solar spectrum in the UV region.

As a well-known photocatalyst, ZnO has been paid much attention in the degradation and complete mineralization of environmental pollutants. Since ZnO has approximately the same band gap energy (3.2 eV) as TiO_2, its photocatalytic capacity is anticipated to be similar to that of TiO_2. However, the greatest advantage of ZnO is that it absorbs large fraction of the solar spectrum and more light quanta than TiO_2 [6]. Some researches have highlighted the performance of ZnO on degrading some organic compounds [6,7]. On the other hand, the use of conventional powder catalyst results in disadvantages in stirring during the reaction and in the separation of powder after the reaction. Preparation of film catalysts will make it possible to overcome these disadvantages and to extend the industrial applications [8]. ZnO thin films have been found to decompose aqueous solutions of reactive dyes [9–11], as well as phenol and chlorophenol [12], and other environmental pollutants.

The sol–gel process, as a simple and easy dip-coating means, is one of the versatile methods to prepare thin film-supported nanosized particles without complicated instruments such as CVD. Thin film photocatalysts, with their high photocatalytic ability, high stability, and convenient reuse, have received more and more attention. However, some problems may be encountered during the sol–gel fabrication of ZnO films. First, more coating times were usually needed to obtain thick layer for an efficient photocatalyst. Thus, inhomogeneous and defects may be introduced, which would affect the properties of the final films. Second, it is difficult to prepare films without peeling off or cracking after calcinations process due to the shrinkage of the films with thermal treatment. Efforts have been made to overcome the above difficulties. Prominently, the sol–gel polymer–inorganic hybrid route is attractive and capable of producing not only thick enough coatings without cracking but also films with novel properties [13,14]. In this case, polymerized materials are mixed into the sol–gel precursors to avoid particle aggregation, to adjust the viscosity of sol, to increase the strength of materials and to prevent crack formation.

In continuation of our ongoing programme to develop thin solid films for photocatalytic purposes [15–17], in the present study we report the preparation of the ZnO covering solution using methylcellulose (MC) as dispersant on slide glass by sol–gel single spin-coating process for photocatalytic decolorization of textile dyes. MC is a water-soluble long chain polymer which is suitable for use in sol–gel processing with high water content. Another advantage is that MC belongs to nonionic cellulose ether, which is substantially free of substance that can induce crystallization of ZnO during any of the coating formation and densification process steps [18]. Using MC as a dispersant we have solved some problems such as inhomogeneity and defects that may be introduced by peeling off and cracking after calcination due to the shrinkage of the films with thermal treatment. The photocatalytic properties of this film toward Acid Blue R (C.I. Acid Blue 92) degradation were investigated and compared with similar ZnO thin film without MC. We have examined the effect of some parameters such as MC content, dye concentration and solution pH on the photodegradation rate.

2. Experimental

2.1. Materials

For the preparation of zinc sol, the following materials and reagents are used: zinc acetate dihydrate (Aldrich, 98%, $Zn(OOCCH_3)_2{\cdot}2H_2O$), acetic acid (Merck) and an ammonia solution (Merck, p.a. NH_3 ca. 25% in H_2O). Methylcellulose (low substitution) was obtained from Harris Chemical. The water used in the experiments was double distilled deionized. For photocatalytic investigation Acid Blue R dye (C. I. Acid Blue 92) was obtained from STIE (China) and has the chemical structure shown in Fig. 1.

2.2. Preparation of MC/ZnO composite materials

Zinc acetate dihydrate (0.3658 g) was dissolved in a mixture of 0.295 ml acetic acid (HAC) and 1.765 ml EtOH, and the solution was agitated for homogenization. Distilled water (2.35 ml) was added to this solution dropwise, under continuous hard stirring for

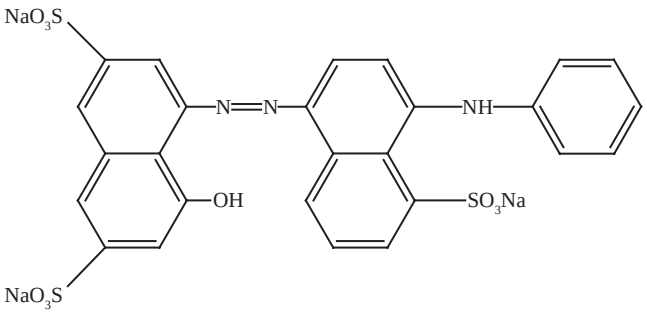

Fig. 1. Chemical structure of commercial diazo dye of Acid Blue R.

several hours. The sol preparation process was exothermic, and the pH was adjusted to 4.2 by adding 5% ammonium hydroxide solution. The molar ratio was adjusted as $Zn(CH_3COO)_2$:HAC:EtOH:H_2O =1:3:18:77. In a separated container, methylcellulose solution (2 wt.% in water) was prepared by dissolving 0.0287 g MC with 1.41 ml distilled water. Both of the prepared solutions (Zn precursor and MC solution) were subsequently mixed and stirred for about 30 h at room temperature. Different precursor solutions have been prepared in order to investigate the influence of MC content on the film properties.

2.3. Deposition of MC/ZnO composite films

Spin coating was utilized to form the films through a three step procedure: (a) the substrate was covered with an excess of solution; (b) the stage and the attached substrate (commonly by vacuum) were accelerated to a prefixed speed and the liquid is evenly distributed on the substrate by the centrifugal force, the liquid in excess being thrown off; (c) the solvent evaporated. The MC/ZnO sol–gel films were spun on the microscope glass slide (75 mm × 25 mm × 1 mm) by a homemade spin coater at room temperature. The speed and the deposition time in step (b) were fixed: 18 s at 1,200 rpm. It should be noted that cleaning the substrate is important for proper adhesion of the films. Microscope glass slide substrates were ultrasonically cleaned in acetone and ethanol. They were then rinsed with deionized water, and dried with pure nitrogen. A 0.22 μm pore sinter glass filter was used to remove foreign particles before the solution was applied to the substrate. After drying at room temperature in air, the films were then baked for about 60 min at each temperature 550°C to develop the crystalline structure in the films during annealing. Fig. 2 shows the flow chart of the preparation of the MC/ZnO composite films.

2.2. Characterization methods

Structural information about both of the dried and heated treated gels was obtained by FTIR (JASCO FT/IR-680 plus). In order to examine the thermal properties of the composite materials, a METTLER TA5 was used for TGA measurement of the gel powder of the composite materials. Microstructure of the prepared samples, were studied by a Philips XL30 scanning electron microscope. The phase composition of the deposited films was studied by plate XRD technique on a D8 Advanced Bruker X-ray diffractometer using Cu Kα radiation at an angle of 2θ from 15 to 60° using a scan speed of 0.03 $2\theta.S^{-1}$. The strongest peaks of ZnO corresponding to Zincite (002) were selected to evaluate the

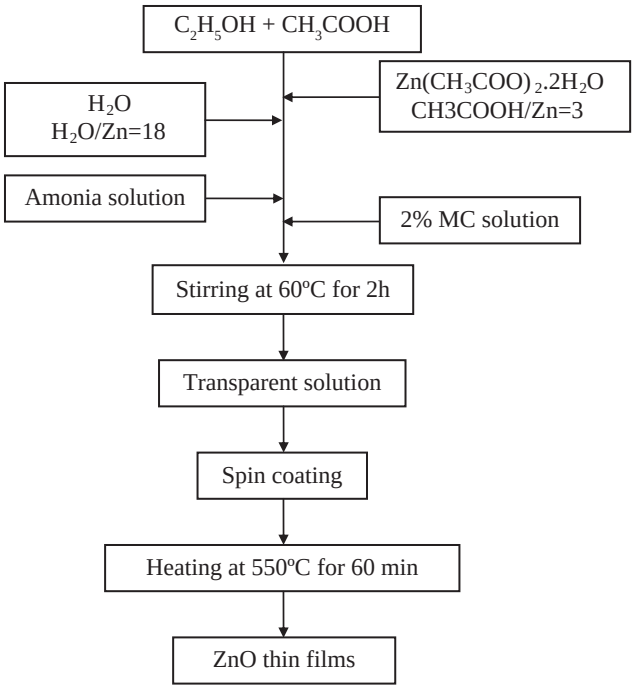

Fig. 2. Flow diagram for preparation of MC/ZnO composite films.

crystallinity of the samples. The mean crystallite size L was determined from the broadening β of the most intense line, for each polymorph, in the X-ray diffraction pattern, based on the Scherer equation:

$$L = \frac{k\lambda}{\beta \cos\theta}$$

where λ is the radiation wavelength, $k = 0.90$ and θ is the Bragg angle. Optical transmittance was measured by a Varian Cary 500 Scan spectrophotometer.

2.5. Photoreactor and photocatalytic measurements

To evaluate the catalytic activity of ZnO thin films, the photodegradation of a well-known organic azo dye Acid Blue R (C.I. Acid Blue 92) is investigated as a simple model compound (Fig. 1) under UV irradiation. The experiments were carried out in a custom made photocatalytic oxidation reactor measured by 80 cm × 50 cm × 50 cm. One ZnO/glass with one time spin-coating (75 mm × 25 mm × 1 mm) was used as photocatalyst and irradiated with one 200 W high-pressure mercury lamp at a distance of 15 cm from the top of the model solution. In all experiment, 10 ml of dye solution with initial concentration of 5 ppm was used. The solution was stirred continuously and a constant-temperature water bath was maintained at 25°C. Four milliliters of the sample was taken at

regular time intervals during irradiation and analyzed by a double beam UV-vis spectrophotometer (UV-2550 UV-visible Spectrophotometer SHIMADZU) to measure the concentration of dye at 580 nm.

3. Results and discussion

3.1. Stability of sol

Type of the zinc sol, reported in this study, with the $Zn(CH_3COO)_2$:HAC:EtOH:H_2O molar ratio of 1:3:18:77, was found to be most suitable for dissolving MC. Different compositions of the sol were prepared by altering the molar ratio of $Zn(CH_3COO)_2$:HAC:H_2O. It was observed that dilution of the sol system may retard the precipitation. The pH of the solution was about 3–4 and MC acts as a dispersant and it retard the precipitation. MC was added to keep the sol solutions stable and clear for a long period (more than 30 days).

3.2. Thermal analysis of the dried MC/ZnO gel

Figs. 3(a) and (b) show FTIR spectra which reveal information about the gel powder of MC/ZnO, before and after heat treatment at 550°C, respectively. The FTIR spectra illustrate a series of absorption bands in the range of 400–4,000 cm^{-1}. The peaks at 1,100–1,800 and 3,200 cm^{-1} in the gel powder of MC/ZnO before heat treatment show that there are significant amounts of water and carbonaceous materials such as MC, whose presence was also reported by other authors [19,20]. Fig. 3(b) shows the spectrum of the product after heat treatment (550°C). Only Zn–O vibrations below 800 cm^{-1} are observed indicating that the material consists of pure ZnO [21,22]. The features vanished after a heat treatment at 550°C, attributing to the burning reaction of organic additives in the heating process.

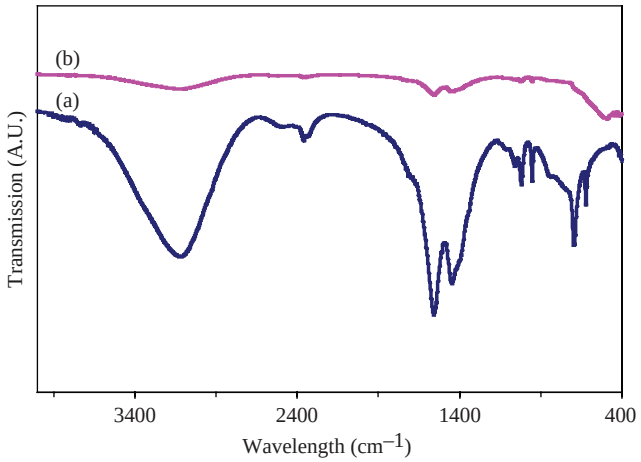

Fig. 3. FTIR spectra of the gel powder of MC/ZnO (a) before (b) after heat treatment at 550°C.

Fig. 4 shows the TGA curve (heating rate 5°C/min) of the gel powder of MC/ZnO in oxygen atmosphere over the temperature range of 50–700°C. The weight loss occurs at three stages, including, below 190°C, between 190 and 230°C and from 230 to 540°C. In the first region (below 190°C), the weight loss is believed to be a result of the evaporation of water and the thermal decomposition of the remnant organic solvents. Between 190 and 230°C, the weight loss is attributed to the carbonization or the combustion of organic compounds such as MC in the composite. Between 230 and 540°C or more, the weight losses are probably ascribed to the evaporation of physically absorbed water and further combustion of the remaining organic additives. Upon further heating beyond this temperature, the weight loss decreases very slowly. This suggests that the organics materials completely have be removed by oxidation in oxygen atmosphere.

3.3. X-ray diffraction analysis

Fig. 5 shows X-ray diffraction (XRD) patterns of the sol–gel derived ZnO nanopowder with MC fired at temperature 550°C for 1 h. A sol–gel derived ZnO nanopowder without MC is also showed as a reference. For the sol–gel derived ZnO nanopowder with MC, diffraction lines can be clearly observed at 2θ = 31.76°, 34.39° and 36.24°, corresponding to 100, 002, 101 reflections of the wurtzite structure, respectively. Diffraction peaks can also be seen in the same positions for the sol–gel derived ZnO nanopowder without MC, showing that MC is substantially free of substance that can induce crystallization of ZnO during any of the coating formation and densification process steps. For the two samples prepared at the temperature of 550°C, (1 0 0), (1 0 1) and (0 0 2) peaks are all very strong in the XRD pattern. This demonstrates the weak

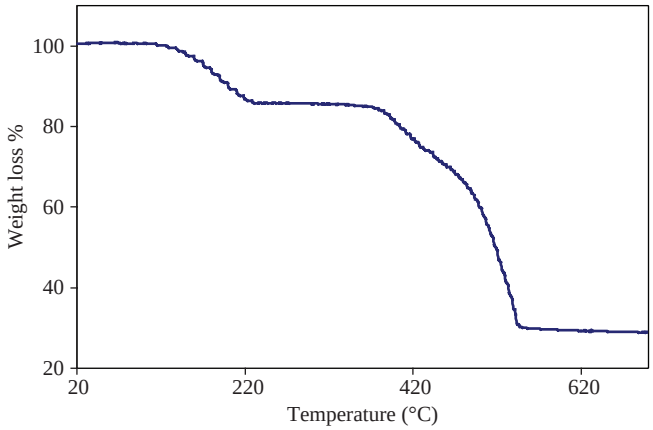

Fig. 4. TGA curve of the gel powder of MC/ZnO composite material.

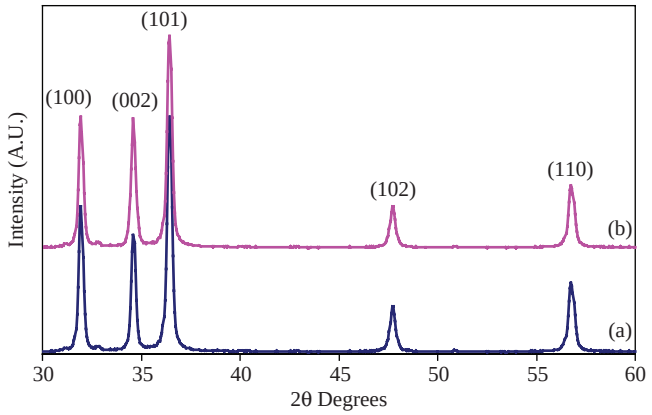

Fig. 5. XRD patterns of the sol–gel derived ZnO nanopowder fried at 550°C for 1 h (a) without MC, (b) with MC.

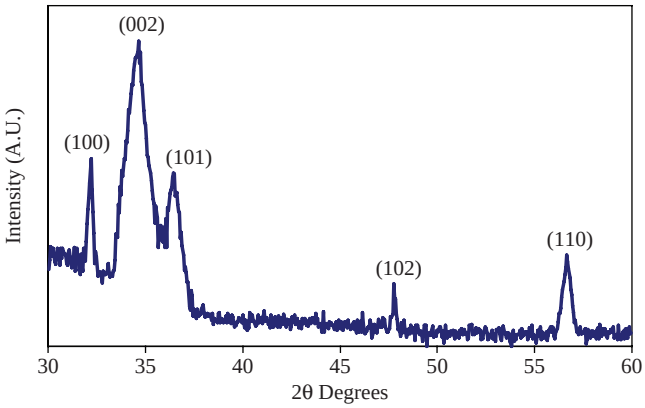

Fig. 6. XRD pattern of the MC/ZnO films fried at 550°C for 1 h.

preferential growth of ZnO grains and confirms the grains have freely grown along different directions.

Fig. 6 shows XRD pattern of ZnO film obtained after the calcination of MC/ZnO composite film at 550°C. This pattern easily confirms zinc oxide structure of the film. The low intensity of the ZnO peaks can be explained by the low flux of the incident beam and the small thickness of the film. It is observed in the XRD pattern of nanopowder samples (Fig. 5) that the (1 0 0) and (1 0 1) diffraction peaks have lower intensity compared with the (0 0 2) peak, according to the standard card. The ZnO films grow with a (0 0 2) orientation is kinetically preferred, which in turn likely reflects the fact that the highest density of Zn atoms is found along the (0 0 2) plane [23].

The average crystallite sizes of ZnO were calculated by Scherrer's equation using the full width at half maximum (FWHM) of the X-ray diffraction peaks at $2\theta = 34.39$. The average crystalline size have been calculated to be in the range of 15–16 nm for MC/ZnO in the films annealed at 550°C. The average crystalline size of ZnO in the powder, either with or without MC, annealed at 550°C was in the range 21–22 nm.

3.4. Surface morphology

Thermal calcination (at 550°C, for 1 h) of as-deposited films led to inorganic transparent nanocrystalline films of ZnO. The main aim of the thermal treatment was to remove the organic part. The thermogravimetric measurement of MC revealed 100% weight loss above 400°C [24]. In our experiments, a temperature of 550°C and time of calcination lasting 1 h were sufficient to remove the organic phase from the as-deposited films. Different MC concentrations in the starting solutions are tested to obtain films of different thicknesses. On a large scale, films do not exhibit stained textures after spinning. Figs. 7(a) and 7(b) illustrate the SEM images of ZnO films obtained after the calcinations of the as-deposited film without (Fig. 7a) and with (Fig. 7b) MC. The SEM image of ZnO film obtained without MC shows particles of ZnO in the range of 60–80 nm. The surface of the ZnO film obtained with the highest amount of MC (theoretically 10 wt% of ZnO) shows smaller ZnO particle sizes—between 20 and 40 nm. Surfaces are without cracks and voids and are quite smooth.

As shown, the average size of ZnO crystallites in powder calculated by Scherrer's equation with and without MC is 15–16 nm and 21–22 nm, respectively. The size of ZnO particles obtained from SEM is relatively larger than the crystallite size calculated from the X-ray method, but this is a well-known phenomenon.

The SEM images clearly indicate the influence of MC on the film morphology. In the nanocomposite with a great amount of MC, the growth of nanoparticles seems more inhibited, and proper deposition conditions for nanocomposite films are achieved. This may occur due to an adequate raise of viscosity during film deposition (i.e., spin coating), solvent evaporation, and the enhancement of the affinity between water and the substrate. Fig. 7b demonstrates the introduction of MC has affected the surface morphology and roughness of films.

3.5. Photocatalytic activity

Prior to the photocatalytic degradation of Acid Blue R in the presence of the ZnO layers, control tests in similar experimental conditions but without the active layer or in dark have been performed. Fig. 9(♦) clearly shows that the direct photolysis of the dye is ineffective leading to a photodegradation degree less than 10%, after a reaction time of 60 min. The results in the dark confirmed that the removal of dye was insignificant for the mentioned condition.

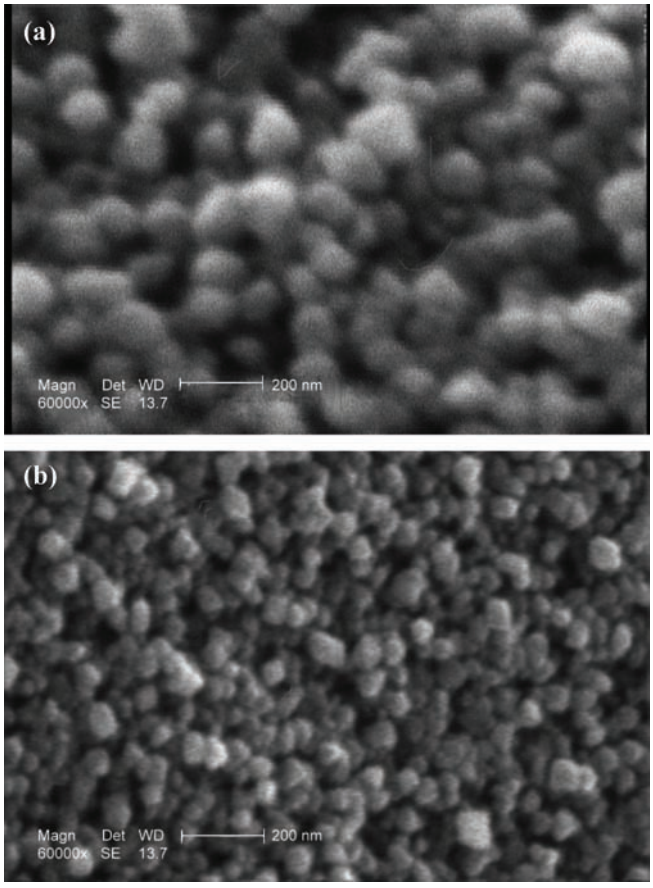

Fig. 7. SEM images of the ZnO films after heat treatment at 550°C for 1 h (a) without MC (b) with MC.

By contrast an effective decoloration is observed when Acid Blue R solutions are in contact with MC/ZnO film under UV exposure, as seen in Fig. 8. It shows a typical time-dependent UV-vis spectrum of Acid Blue R solution during photoirradiation on 2%MC/ZnO thin film after heat treatment at 500°C. The spectrum of the dye in the visible region exhibits a main band with a maximum at 580 nm. The absorption peaks, corresponding to color of dye at $\lambda_{max} = 580$ and another, corresponding to Π–Π* transition of aromatic rings of dye at 265 nm were diminished and finally disappeared under reaction which indicated that the dye had been degraded. No new absorption bands appear in the visible or ultraviolet regions. The presence of the ZnO thin film without MC (Fig. 9 (■)) and ZnO thin film with MC (Fig. 9 (▲)) resulted in an effective photocatalytic degradation of the azo dye. The ratio A/A_0 gives the intensity attenuation of the characteristic band of the dye whose maximum is located at 580 nm ($\lambda_{max} = 580$ nm). These results show that the ZnO films are very effective in photodegrading Acid Blue R, as denoted by the decrease of the band intensity ($\lambda_{max} = 580$ nm) with running reaction time

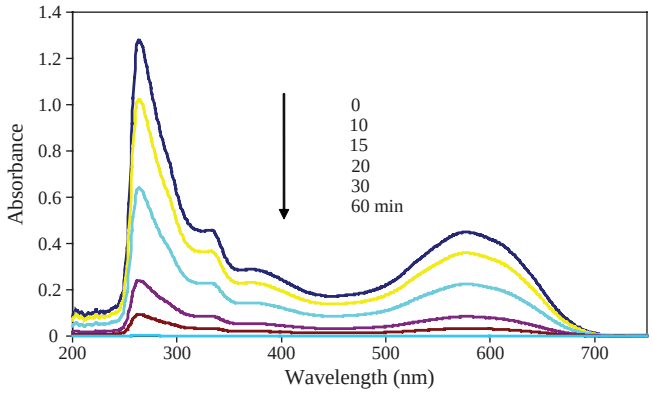

Fig. 8. Time-dependent UV-vis spectrum of Acid blue R solution during photoirradiation on 2%MC/ZnO thin film after 1 h heat treatment at 550°C; pH, 6.0; one time coating; dye concentration, 5 ppm.

(~99% after 60 min for MC/ZnO; (~88% after 60 min for ZnO).

Following the methodology proposed by different authors [9,25–26], and also checked by us, the results allow a semi-quantitative analysis by comparing the apparent rate constants of the photodegradation reactions. In these conditions, generally the photocatalytic reaction follows a Langmuir–Hinshelwood mechanism with the reaction rate being proportional to the photocatalytic material coverage with the dye molecules. The linear transforms $\ln(A_0/A) = k_a t$ of the curves in Fig. 9 are given in Fig. 10. In general a good correlation was obtained (>0.97), suggesting that the reaction kinetics follows a pseudo-first order rate law. The slopes of the straight lines passing through the origin yield the apparent rate constants (k_a) depicted in Table 1. This table also shows the maximum percentage decoloration (A/A_0) and half-time values ($t_{1/2}$), corresponding to the time for which the dye is reduced to half of

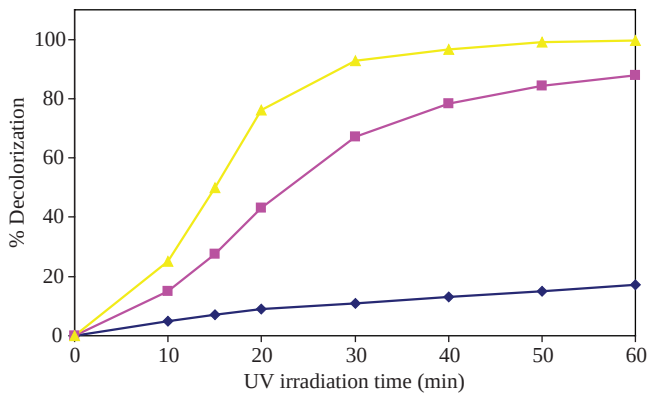

Fig. 9. Degradation of Acid Blue R solution without photocatalyst (♦), in the presence of ZnO thin film without (■) and with MC (▲).

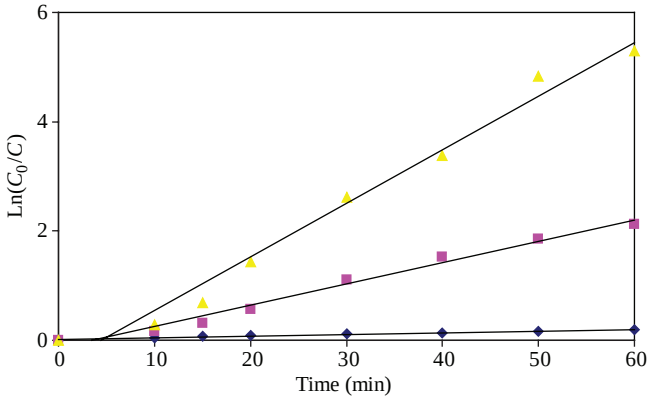

Fig. 10. The kinetic data for photocatalytic degradation of Acid Blue R in without photocatalyst (◆), in the presence of ZnO thin film without (■) and with MC (▲).

the initial amount. As can be seen from Table 1, the photocatalytic activity is enhanced when the MC are introduced in the catalyst. We attribute the relatively higher photocatalytic activity of the composite to increase roughness of films. Fig. 7b shows that the introduction of MC has decreased the ZnO particle size and increased the surface morphology and roughness of films. These results indicate that although the addition of MC can enhance the photocatalytic activity of ZnO thin films, with using 2.5% MC, photocatalytic activity of ZnO thin films have been decreased. The optimal amount of MC was obtained 2%.

The evaluation of experimental variables, namely the concentration of dye and pH of the solution, was studied within reasonable limits. It shows that the treatment of higher concentrated Acid Blue R solutions (10 mg/L) is less effective, as predicted from the existence of a higher relative amount of dye molecules to be degraded by an equal and fixed number of active sites in the layer, while the photocatalytic degradation of the lower concentrated dye solutions (1–5 mg/L) is raised with increase dye concentration, due to existence of a lower amount of dye molecules to be degraded by fixed number of active sites on the film.

The pH is an important parameter for photocatalytic processes. The properties of solid–electrolyte interference, i.e. the electrical double layer, can get modified as the pH of the medium changes. Consequently, the effectiveness of the adsorption–desorption process and the separation of the photogenerated electron–hole pair are also substantially affected [26,27]. In present system with an increase in pH from 3 to 5, the reaction rate is increased. At pH 5, the maximum initial rate is achieved and with further increase in pH, the rate of photo degradation decreases. The low initial reaction rates at acidic or at alkali pH values are due to dissolution and photodissolution of ZnO [28]. The semiconductor ZnO is amphoteric in nature. At acidic pH, ZnO can react with acids to produce the corresponding salt, while at alkaline pH, it can react with a base to form complexes like $[Zn(OH)_4]^{2-}$. The optimal pH was around 5.0, which is the natural value of the aqueous dye solution.

4. Conclusion

ZnO coatings have been successfully prepared by the MC assisted sol–gel and single spin coating process. Crack-free films of ZnO nanoparticles were formed after being heating at 550°C. XRD investigation indicates the formation of wurzite phase after the thermal treatment over 550°C. ZnO layers proved to show interesting Acid Blue R decoloration performance under direct exposure to UV. Maximal color attenuation degree for 2%MC/ZnO thin film is about 98% and decoloration rate, assuming an apparent first order reaction, reached 9.8×10^{-2} min^{-1}. In the actual conditions, MC/ZnO films show superior performance than ZnO. The efficiency of decoloration increased as initial dye concentration decreased. The optimal dye concentration was 10 ppm, with one 2%MC/ZnO thin film.

Table 1
Rate constants (k_a) of Acid Blue R (20 ml, 5 mg/L) photocatalytic decolouration in contact with MC/ZnO and ZnO films on microscope glass slides. Maximum decoloration (%) and half-time ($t_{1/2}$) values are also given

Catalyst	Rate constant (min^{-1})	Decoloration (%)	Half-time (min)
Without photocatalyst	0.0018	10	385
ZnO thin film	0.039	88	17.8
0.5%MC/ZnO thin film	0.039	88	17.8
1%MC/ZnO thin film	0.045	92	15.4
1.5%MC/ZnO thin film	0.055	94	12.6
2%MC/ZnO thin film	0.098	99	7
2.5%MC/ZnO thin film	0.065	96	11

The optimal pH was around 5, which was an available pH of the dye solution.

Acknowledgment

Grateful acknowledgements to the Islamic Azad University, Najafabad Branch and Payame Noor University of Isfahan for the financial support of this work.

References

[1] C. Galindo, P. Jacques and A. Kalt, Chemosphere, 45 (2001) 997–1005.
[2] J.-M. Herrmann, C. Guillard and P. Pichat, Catal. Today, 17 (1993) 7–20.
[3] C.A.K. Gouvea, F. Wypych, S.G. Moraes, N. Duran, N. Nagata and P. Peralta-Zamora, Chemosphere, 40 (2000) 433.
[4] S.I. Abou-Elela and M.A. El-Khateeb, Desalination Water Treat., 7 (2009) 1–5.
[5] T. Sauer, G.C. Neto, H.J. Jose and R.F.P.M. Moreira, Kinetics of photocatalytic degradation of reactive dyes in a TiO_2 slurry reactor, J. Photochem. Photobiol. A: Chem., 149 (2002) 147–154.
[6] S. Sakthivel, B. Neppolian, M. V. Shankar, B. Arabindoo, M. Palanichamy and, V. Murugesan, Solar photocatalytic degradation of azo dyes: comparison of photocatalytic efficiency of ZnO and TiO_2, Sol. Energy Mater. Sol. Cells, 77 (2003) 65–82.
[7] B. Pare, S.B. Jonnalagadda, H. Tomar, P. Singh and V.W. Bhagwat, Desalination, 232 (2008) 80–90.
[8] K. Iketani, R.-D. Sun, M. Toki, K. Hirota and O. Yamaguchi, Mater. Sci. Eng. B, 108 (2004) 187–193.
[9] M. H. Habibi and M. Khaledi, J. Nanomater. ID 356765 (2008) 5.
[10] C.A.K. Gouvêa, F. Wypych, S.G. Moraes, N. Durán, N. Nagata and P. Peralta-Zamora, Chemosphere, 40 (2000) 433.
[11] C. Lizama, J. Ferrer, J. Baeza and H.D. Mansilla, Catal. Today, 76(2002) 235–246.
[12] S. Lathasree, A.N. Rao, B. Siva-Sankar, B. Sadasivam and K. Rengaraj, J. Mol. Catal. A: Chem., 223 (2004) 101.
[13] L. Liu, Q. Lu, J. Yin, Z. Zhu, D. Pan and Z. Wang, Mater. Sci. Eng., C22 (2002) 61–65.
[14] S. Takenaka and H. Kozuka, Appl. Phys. Lett., 79 (2001) 3485–3487.
[15] M. H. Habibi and M. Nasr-Esfahani, Dyes Pig., 75 (2006) 714–722.
[16] M. Nasr-Esfahani and M.H. Habibi, Inter. J. Photoenergy, (2008), Article ID 628713, 11.
[17] M. Nasr-Esfahani and M.H. Habibi, Desalination Water Treat., 3 (2009) 64–72.
[18] R.A. Caruso and J.H. Schattka, Adv. Mater., 24 (2000) 1921–1923.
[19] C.J. Kang, J.S. Chun and W.J. Lee, Thin Solid Films, 189 (1990) 161–173.
[20] B.M. Keyes, L. M. Gedvilas, X. Li and T. J. Coutts, J. Cryst. Growth, 281 (2005) 297–302.
[21] D. Mondelaers, G. Vanhoyland, H. Vandenrul, J. D'Haen, M.K. Vanbael, J. Mullens and L.C. Vanpoucke, J. Sol-Gel Sci. Techn., 26 (2003) 523–526.
[22] P. R. Patil and S. S. Joshi, Mater. Phys., 105 (2007) 354–61.
[23] S. Amirhaghi, V. Cracium, D. Cracium, J. Elders and I. W. Boyd, Microelectron. Eng., 25 (1994) 321–326.
[24] M.H. Habibi, M. Nasr-Esfahani and T.A. Egerton, J. Mater. Sci., 42 (2007) 6027–6035.
[25] J.R. Bellobona, A. Carrana, B. Barni and A. Gazzotti, J. Photochem. Photobiol. A: Chem., 84 (1994) 83–90.
[26] J. Marto, P. São Marcos, T. Trindade and J.A. Labrincha, J. Hazard. Mater., 163 (2009) 36–42.
[27] E. Evgenidou, K. Fytianos and I. Poulios, J. Photochem. Photobiol. A: Chem., 175 (2005) 29–38.
[28] N. Daneshvar, D. Salari and A.R. Khataee, J. Photochem. Photobiol. A: Chem., 162 (2004) 317–322.